A novel adaptive control scheme for dynamic voltage restorer

Tummala Kranti Kiran[1], Balakrishnan Rajagopal[1], Yerramilli Butchi Raju[2]
[1]Department of Electrical Engineering, Annamalai University, Chidambaram, India
[2]Department of Electrical and Electronic Engineering, Sir C. R. Reddy College of Engineering, Eluru, India

Article Info	ABSTRACT
	This study introduces a novel approach to improve the performance of the dynamic voltage restorer (DVR) using a control structure based on the inverse hyperbolic sine function-based least mean square (IHSF-LMS). The proposed control structure efficiently extracts the fundamental source voltage component with rapid convergence. The primary objective of this control scheme is to enhance compensation capability and maintain load voltage stability. Key features include superior steady-state performance and heightened robustness with reduced computational complexity. This approach achieves a reduction in peak overshoot and settling time compared to the traditional LMS method. The validation of system performance is conducted through MATLAB/Simulink simulations, demonstrating compliance with the IEEE-519-2014 standards for harmonic spectra.

Corresponding Author:

Tummala Kranti Kiran
Department of Electrical Engineering, Annamalai University
Annamalainagar 608002, Chidambaram, Tamil Nadu, India
Email: krantikiran.tummala@gmail.com

1. INTRODUCTION

Power electronic devices have gained popularity in both consumer and industrial sectors due to advantages such as energy conservation, cost-effectiveness, smaller size, and reduced maintenance requirements [1], [2]. However, these devices introduce power quality concerns, including voltage sag, swell, unbalancing, and distortions at the distribution end. These issues lead to undesirable consequences such as increased losses and malfunctioning protective equipment. Power quality (PQ) problems are prevalent in distribution networks and pose significant challenges [3]. Addressing these concerns, [4] provides a list of custom power devices (CPDs) designed to enhance PQ in distribution networks. In a study by Das *et al.* [5], a brief overview of deteriorating power quality is presented. Within the realm of power quality, a series-connected device referred to as the dynamic voltage restorer (DVR) has been introduced to address voltage-related issues [6].

The control strategy implemented in the DVR significantly influences operational performance during various disturbances in grid voltages. Preview study [7], [8] proposed software PLL (SPLL) for DVR control, focusing on estimating phase jumps during system faults to protect loads. The basic control scheme is a synchronous reference frame (SRF), which is implemented for DVR for mitigation of voltage sag and swell [9], [10]. However, its complexity arises from inherent abc/dq transformations and the presence of a phase lock loop [11], potentially introducing errors if the SRF is not identified accurately. The dual-pq theory-based DVR with embedded EZ source inverter topology is articulated in [12]. Various filtering techniques, such as modified dual-second-order generalized integrator (MD-SOGI) [13], least mean square (LMS) [14], and least mean fourth (LMF), among others, are available in the literature. The distinct comparison between LMS, LMF, and combined LMS/F is made by the author in [15], indicating the capability of the LMS/F-based control algorithm. However, it is noted that the LMS algorithm is susceptible

to optimization errors and increased computational burden, while the LMF algorithm exhibits a poor steady-state response, focusing primarily on dynamic response. Furthermore, the combined LMS LMF-based control scheme overcomes the shortfalls of the LMS control technique, such as a lower convergence rate [16]. To handle voltage distortions and unbalances, the recursive least squares (RLS) technique is implemented for DVR operation [17]. The second-order generalized integrator (SOGI) algorithm has limitations in DC offset rejection and performance degradation during a distorted grid state. Preview study [18], a frequency adaptive enhanced reduced-order generalized integrator (FAEROGI)-based control algorithm is implemented for DVR operation. The FAEROGI-based control scheme offers notable benefits, including reduced settling time, lower peak overshoot, and faster-unbalanced compensation.

The effectiveness of adaptive filters heavily relies on the selection of an appropriate cost function, a critical factor in diverse noise environments [19]. To achieve superior steady-state alignment and enhanced robustness in impulsive noise conditions, a generalized hyperbolic secant cost function has been employed [20]. Similarly, the arctangent cost function has been integrated into the normalized least mean square (NLMS) framework, demonstrating heightened resilience against impulsive interference [21]. A multi-convex adaptive least mean square (LMS) filter-based control strategy is proposed in [22] for DVR applications, where each LMS sub-filter excels in harmonic suppression and dynamic tracking by utilizing step-size adaptation for superior voltage distortion management. Further advancements are seen in [23], where a modified fractional least mean square (M-FLMS) control scheme optimizes DVR performance. By incorporating an adjustable gain parameter into the original FLMS structure, the M-FLMS method achieves faster convergence, reduced steady-state errors, and higher computational efficiency during voltage distortions. Alternatively, transformer-based impedance source inverters (Trans-Z source inverters) have been explored for DVR operation in [24]. Notably, while methods in [21]–[23] showcase improved robustness and performance metrics, they are accompanied by higher computational demands. Therefore, there is a need for an algorithm with a novel cost function that delivers both robust steady-state and dynamic responses, even under unbalanced grid conditions, ensuring appropriate DVR operation. In [25], a study employed the inverse hyperbolic sine function as a cost function, showcasing improved steady-state accomplishment and increased resilience against impulsive interference when compared to several existing algorithms. Hence, this work refers [25] to the effective operation of DVR.

The prime contributions of the technical manuscript are: i) The IHSF-LMS-based control scheme is utilized for the efficient extraction of the fundamental component (FC) from a distorted source voltage. It offers improved steady-state performance and demonstrates strong resilience to impulsive interference. Additionally, its implementation is straightforward, eliminating the need for complex mathematical computations; ii) A comparative analysis between the proposed IHSF-LMS control scheme and the traditional LMS technique highlights its superior performance. Notably, the proposed algorithm's computational burden is significantly lower than the methods discussed in [21]–[23]; iii) The proposed control algorithm effectively ensures that the total harmonic distortion (THD) of the load voltage remains well within acceptable limits, complying with the 5% threshold specified in the IEEE-519-2014 standard.

2. DVR CONFIGURATION

Figure 1 illustrates the MATLAB/Simulink model of the 3P3W-VSC-based DVR configuration with a capacitor support. The major portion includes a three-phase supply with distortions created, such as voltage sag, swell, distortions, and imbalance, and the three-phase-sensitive load, which needs to be protected from these undesirable changes in supply voltage. The DC-link capacitor provides voltage as input during different disturbances. The filter has been used at the output of the voltage source converter (VSC) to remove switching harmonics generated by the VSC. The voltage is to be inserted into the system through a single-phase series-connected injection transformer. The supply voltage is represented by v_{sabc} and the load voltage as well as the currents are depicted as v_{Labc} and i_{Labc}, respectively. V_{DC} is the DC-link voltage across the capacitor and v_{cabc} is the DVR-injected voltage during the disturbances.

3. IHSF-LMS BASED-CONTROL ALGORITHM

The main function of a DVR is to inject a compensating voltage in series with the power supply, maintaining stable voltage regulation at the load terminal. The effectiveness of the control algorithm hinges on isolating the fundamental source voltage component that aligns with the unit load current template. For precise evaluation, the unit load current template must maintain phase synchronization with the load current while exhibiting a unit magnitude.
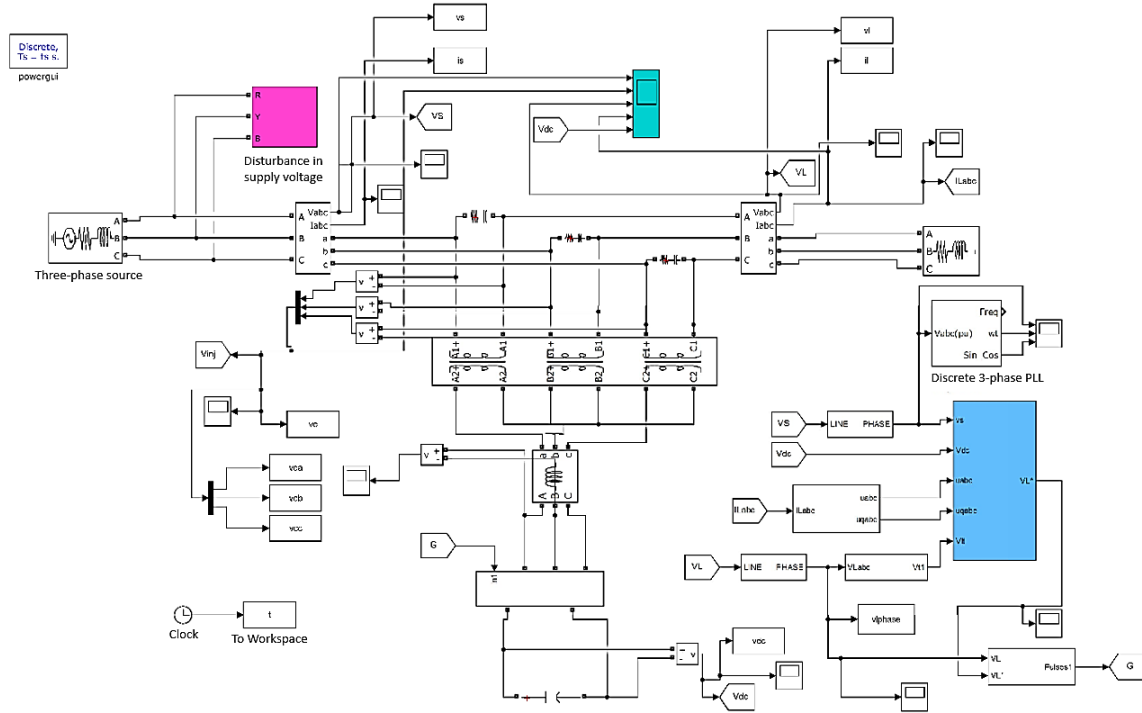
Figure 1. MATLAB/Simulink model of the 3P3W-VSC-based DVR configuration with a capacitor support

3.1. Inverse hyperbolic sine function-based (IHSF) LMS adaptive filtering algorithm

Figure 2(a) illustrates a complete circuit representation of the inverse hyperbolic sine function-based (IHSF) LMS adaptive filtering algorithm for DVR. The IHSF-LMS control-based extractor for phase 'a' is depicted in Figure 2(b). The line voltages are represented as v_{ab} , and v_{bc}. After measuring it at the point of common coupling (PCC), the conversion into phase voltages v_a, v_b and v_c is as (1).

$$\begin{pmatrix} v_a \\ v_b \\ v_c \end{pmatrix} = \frac{1}{3} \begin{bmatrix} 2 & 1 \\ -1 & 1 \\ -1 & -2 \end{bmatrix} \begin{bmatrix} v_{ab} \\ v_{bc} \end{bmatrix} \tag{1}$$

From the power circuit, the load currents will be sensed. Three-phase load current (i_L) is used to determine in-phase and quadrature unit templates. Let I_{La} is the magnitude of the three-phase load current which is given by (2).

$$I_{La} = \sqrt{\frac{2}{3}\left(i^2{}_{La} + i^2{}_{Lb} + i^2{}_{Lc}\right)} \tag{2}$$

The in-phase as well as quadrature unit templates are given by (3) and (4).

$$\left. \begin{aligned} \sigma_{pa}(n) &= \frac{i_{La}}{I_{La}} \\ \sigma_{pb}(n) &= \frac{i_{Lb}}{I_{La}} \\ \sigma_{pc}(n) &= \frac{i_{Lc}}{I_{La}} \end{aligned} \right\} \tag{3}$$

$$\left. \begin{aligned} \sigma_{qa}(n) &= 0.577 * \left[\sigma_{pc}(n) - \sigma_{pb}(n)\right] \\ \sigma_{qb}(n) &= 0.289 * \left[3\sigma_{pa}(n) + \sigma_{pb}(n) - \sigma_{pc}(n)\right] \\ \sigma_{qc}(n) &= 0.289 * \left[-3\sigma_{pa}(n) + \sigma_{pb}(n) - \sigma_{pc}(n)\right] \end{aligned} \right\} \tag{4}$$

The utilized cost function in this context is the inverse hyperbolic sine function (IHSF) with the squared error as its argument, represented by (5).

$$J_{HSF}(e(n)) = E\left[sinh^{-1}(e^2(n))\right] \tag{5}$$

The term $sinh^{-1}[.]$ is inverse hyperbolic sine function. As far as the definition of the IHSF is concerned, it is vigorously convex at $e(n) \in (-\infty, \infty)$. The cost function employed to derive the proposed IHCF adaptive filtering algorithm is expressed as (6).

$$\alpha(n) = argmin J[\alpha(n)] = argmin J\left[sinh^{-1}(e^2(n))\right] \tag{6}$$

Its gradient with respect to the filter coefficient is as (7).

$$\frac{\partial J[\alpha(n)]}{\partial [\alpha(n)]} = \frac{\partial\left[sinh^{-1}(e^2(n))\right]}{\partial [\alpha(n)]} = -2e(n)x(n) \tag{7}$$

Hence, the updated weight equation for IHSF-LMS is as (8).

$$\alpha(n) = \alpha(n-1) + 2\gamma \times \frac{1}{\sqrt{1+e^2(n)}} e(n)x(n) \tag{8}$$

The term γ is adaptation constant and $x(n)$ is input vector. The term $e_{pa(n)}$ in (9) is the error between substantial and fundamental estimated signals. Furthermore, the weight transfer rule for active components of phase 'b' and 'c' is given by (9).

$$\left.\begin{aligned}
\alpha_{p_b}(n) &= \alpha_{p_b}(n-1) + 2\gamma \frac{1}{\sqrt{1+e_{pb}^2(n)}} e_{pb}(n)\sigma_{pb}(n) \\
e_{pb}(n) &= v_{sb}(n) - \sigma_{pb}(n) * \alpha_{pb}(n-1) \\
\alpha_{p_c}(n) &= \alpha_{p_c}(n-1) + 2\gamma \frac{1}{\sqrt{1+e_{pc}^2(n)}} e_{pc}(n)\sigma_{pc}(n) \\
e_{pc}(n) &= v_{sc}(n) - \sigma_{pc}(n) * \alpha_{pc}(n-1)
\end{aligned}\right\} \tag{9}$$

The term α_{sp} is the mean of $\alpha_{pa}(n), \alpha_{pb}(n), \alpha_{pc}(n)$ which active component of all three phases is given by (10).

$$\alpha_{sp} = average(\alpha_{pa}(n), \alpha_{pb}(n), \alpha_{pc}(n)) \tag{10}$$

It represents the mean weight of the fundamental d-axis component in the reference supply voltage. Similarly, the weight transfer rule for a reactive component of phase 'a,' 'b', and 'c' is given by (11).

$$\left.\begin{aligned}
\alpha_{q_a}(n) &= \alpha_{q_a}(n-1) + 2\gamma \frac{1}{\sqrt{1+e_{qa}^2(n)}} e_{qa}(n)\sigma_{qa}(n) \\
e_{qa}(n) &= v_{sa}(n) - \sigma_{qa}(n) * \alpha_{qa}(n-1) \\
\alpha_{q_b}(n) &= \alpha_{q_b}(n-1) + 2\gamma \frac{1}{\sqrt{1+e_{qb}^2(n)}} e_{qb}(n)\sigma_{qb}(n) \\
e_{qb}(n) &= v_{sb}(n) - \sigma_{qb}(n) * \alpha_{qb}(n-1) \\
\alpha_{q_c}(n) &= \alpha_{q_c}(n-1) + 2\gamma \frac{1}{\sqrt{1+e_{qc}^2(n)}} e_{qc}(n)\sigma_{qc}(n) \\
e_{qc}(n) &= v_{sc}(n) - \sigma_{qc}(n) * \alpha_{qc}(n-1)
\end{aligned}\right\} \tag{11}$$

In (11), α_{sq} is the mean of $\alpha_{qa}(n), \alpha_{qb}(n), \alpha_{qc}(n)$ which reactive component of all the three phases and it is given by (12).

$$\alpha_{sq} = average(\alpha_{qa}(n), \alpha_{qb}(n), \alpha_{qc}(n)) \tag{12}$$

It represents the mean weight of the FC of the q-axis in the reference supply voltage. The signal α_{sp} is passed through a LPF that separates the non-oscillating portion. It extracts DC apparatus and harmonics. The error (v_{DCe}) is obtained by subtracting the actual DC-bus voltage V_{DC} from reference DC bus voltage (v_{dc}^*). This is provided to the DC side PI controller. The output of the DC-PI controller is V_{dPI} regulates V_{DC}. The term V_{pd} will be (13).

$$V_{pd} = \alpha_{sp} - V_{dpI} \tag{13}$$

Let the load terminal voltage (v_{Lt}) is obtained through (14).

$$v_{Lt} = \sqrt{\frac{2}{3}(v^2_{La} + v^2_{Lb} + v^2_{Lc})} \qquad (14)$$
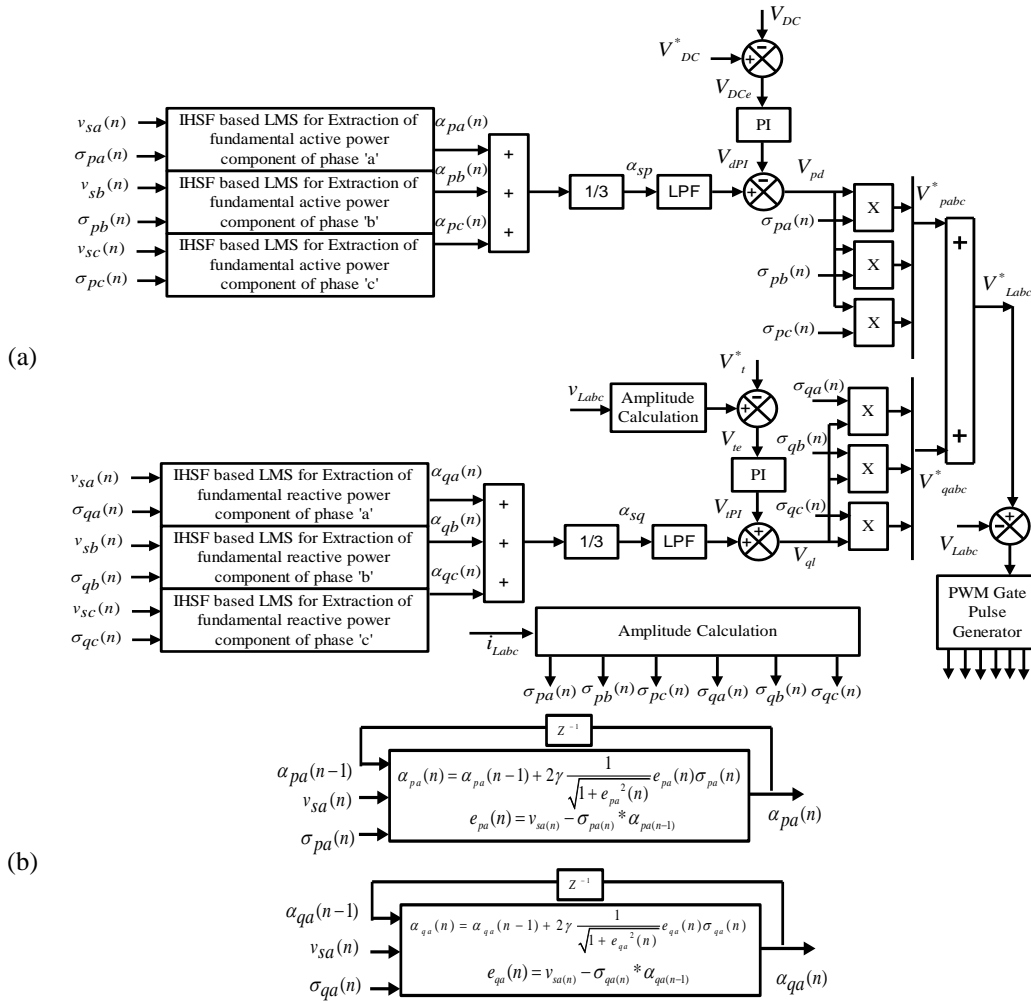

Figure 2. Control diagram of DVR: (a) IHSF-LMS-based control diagram for DVR and (b) IHSF-LMS control algorithm-based extractor

The reference load terminal voltage is (v^*_{Lt}). The v_{Lt} is compared with reference load terminal voltage that generates an error (v_{ter}). The error signal is given to the AC side PI controller which gives v_{LPI} as output. This output is essential to regulate the terminal load voltage of the DVR. α_{sq} is passed through LPF to extract load-reactive components. The output of AC-PI controller v_{LPI} is added to the average three-phase reactive fundamental component α_{sq} that gives signal V_{ql}.

$$V_{ql} = \alpha_{sq} + V_{LPI} \qquad (15)$$

Three-phase active and reactive components of reference voltage v^*_{pabc} and v^*_{qabc} are given by (16) and (17).

$$v^*_{pabc} = V_{pd} * \sigma_{pabc}(n) \qquad (16)$$

$$v^*_{qabc} = V_{ql} * \sigma_{qabc}(n) \qquad (17)$$

The signal (v^*_{Labc}) will be determined with the help of (16) and (17) as (18).

$$v^*_{Labc} = v^*_{pabc} + v^*_{qabc} \qquad (18)$$

The error generated by comparing (v^*_{Labc}) and (v_{Labc}) is utilized for PWM generation.

4. SIMULATION RESULT OF DVR USING IHSF-LMS-BASED ADAPTIVE FILTERING ALGORITHM

The 3P3W DVR utilizing the inverse hyperbolic sine function-based LMS (IHSF-LMS) control algorithm has been modeled and simulated in MATLAB Simulink. A sample time of 20 microseconds was utilized for the simulations. Voltage swell and sag events were applied for durations of $0.4 \leq t \leq 0.48$ s. and $0.54 \leq t \leq 0.62$ s., respectively, while source voltage distortion was introduced over a range of $0.7 \leq t \leq 0.78$ s. Additionally, voltage unbalance was observed at $0.84 \leq t \leq 0.9$ s. The subsequent sections provide a detailed analysis of DVR operation. Intermediate signals are analyzed to assess the DVR's performance under the specified control scheme. Simulation results are discussed in the following sub-sections.

4.1. Intermediate signals of the IHSF-LMS-based control scheme

Figures 3(a) and 3(b) represent the internal signals of IHSF-LMS from the supply voltage of phase 'a' (v_{sa}). The first subplot in Figures 3(a) and 3(b) indicates source side voltage (v_{sabc}) with aforementioned PQ issues. The active FC of the v_{sabc} of phase 'a' is represented by α_{pa} in subplot two. The signal α_{sp} obtained from (10) is the third subplot of Figures 3(a) and 3(b). The term v_{pa}^* calculated from (18) which is the reference active component of load voltage for phase 'a' can be depicted in subplot four. Moreover, the reactive FC of the v_{sabc} with the phase 'a' i.e., α_{qa} is represented by the subplot fifth of Figures 3(a) and 3(b). A signal α_{sq} obtained from (12) is illustrated in the sixth subplot of Figures 3(a) and 3(b). The term v_{qa}^* calculated from (17) which is the reference reactive component of load voltage for phase 'a' is illustrated in subplot seventh. Finally, the reference load voltage obtained from (18) is articulated in subplot eight. From Figures 3(a) and 3(b), it is observed that the offered IHSF-LMS-based control scheme produces a balanced three-phase reference load voltage even though the source voltage is distorted.

4.2. DVR overall performance with IHSF-LMS-based control scheme

Figure 4 demonstrates the comprehensive performance of the DVR using the IHSF-based LMS control technique under various dynamic conditions. Figure 4(a) includes voltage swell and sag conditions, whereas Figure 4(b) includes voltage distortion and unbalanced conditions. For both Figures 4(a) and 4(b), the subplots are the same viz. supply voltages (vsabc), load voltages (vLabc), compensated voltages (vca, vcb, and vcc), load currents (iLabc), and DC-bus voltage (Vdc) and terminal voltage (Vt). From both Figures 4(a) and 4(b), it is noteworthy that the load voltage is balanced and of constant magnitude. This indicates the effectiveness of the proposed control scheme. Harmonic analysis vsabc proposed IHSF-LMS and conventional LMS are shown in Figure 5(a). Significantly improved using the proposed control scheme, achieving 1.61%, compared to 3.03% with the conventional LMS, as illustrated in Figure 5(b). Similarly, the load current THD is reduced to 1.48% for the proposed controller, whereas the conventional LMS achieves 2.05%, as seen in Figure 5(c). These results highlight the superior harmonic mitigation capabilities of the IHSF-LMS controller over the conventional LMS algorithm, particularly in improving the quality of load voltage and current. Additionally, Table 1 provides the simulation performance of the IHSF-based LMS algorithm.
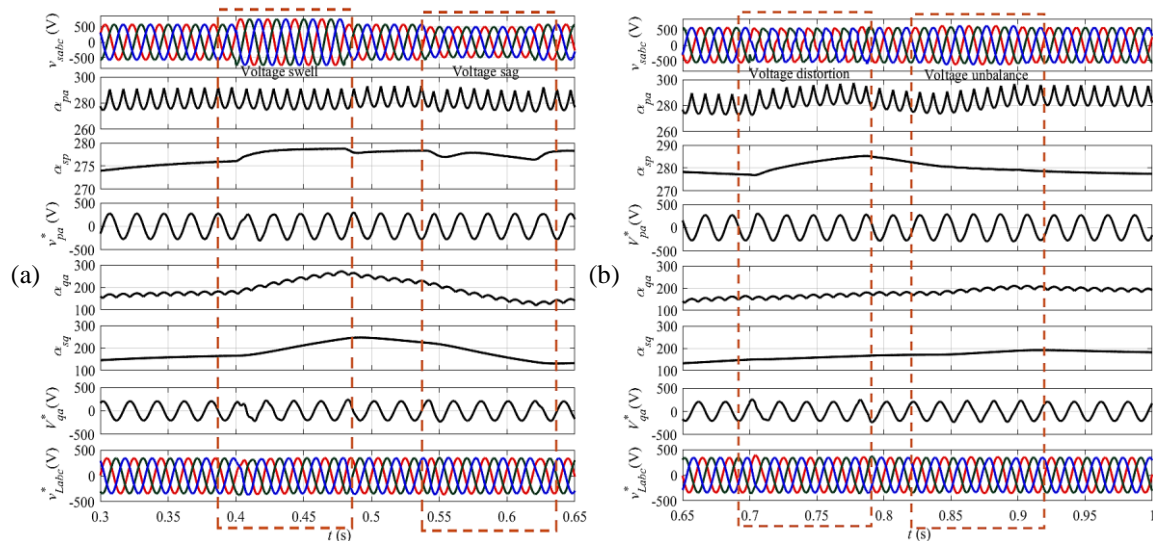

Figure 3. Intermediate signals for proposed IHSF-LMS-based control scheme during: (a) voltage swell and sag and (b) voltage distortion and unbalance
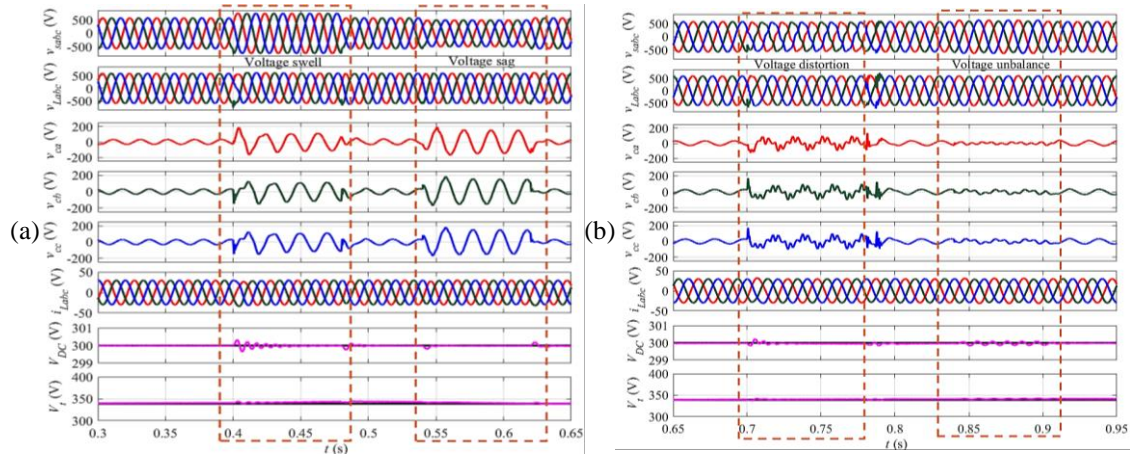
Figure 4. Comprehensive effectiveness of the DVR with the IHSF-LMS control scheme:
(a) voltage swell and sag (b) voltage distortion and voltage unbalance

Table 1. Simulation performance of the IHSF-based LMS algorithm

Sr. No.	Disturbance nature		Parameter in RMS values
1.	DVR behavior	0.82 p.u. sag	v_{sabc} = 339.2 V, v_{cabc} = 75.83 V, v_{Labc} = 415 V
2.	(dynamic condition)	1.2 p.u. swell	v_{sabc} = 443 V, v_{cabc} = 31.54 V, v_{Labc} = 415 V
3.		Distortion	v_{sabc} = 316.4 V, v_{cabc} = 30 V, v_{Labc} = 415 V
4.		Unbalance (resistive load is connected between phases 'a')	v_{sabc} = 415 V, v_{cabc} = 30.68 V, v_{Labc} = 415 V
5.	DVR behavior (steady-state condition)	Voltage distortion	v_{sabc} = 9.79%, v_{Labc} = 9.79 %

5.   COMPARISION OF IHSF-LMS-BASED CONTROL WITH CONVENTIONAL LMS CONTROL TECHNIQUE

        The effectiveness of IHSF-LMS is compared with conventional LMS. The fundamental active weight component of phase 'a' is compared to assess its effectiveness with the LMS and IHSF-LMS-based control schemes. It is depicted in Figure 6. The wave shapes show that there are persistent oscillations with considerable magnitude in the case of the LMS controller. Oscillations with reduced amplitude are observed with the IHSF-LMS controller. It shows that the weight converges faster, and a smaller static error is achieved in steady-state conditions with (t = 0.1 to 0.5 s.) for the proposed IHSF-LMS control scheme. Now, the unbalanced load condition with a time frame of t = 0.8 to t = 0.85 s is considered. It is noteworthy that during dynamic situations, the convergence of the proposed IHSF-LMS-based control technique is better with lesser steady-state error. It shows its effectiveness during voltage anomalies.

        Figures 5(a)-5(c) illustrate the harmonic analysis of load voltage using LMS, IHSF-LMS, and source voltage, respectively. Meanwhile, Figure 7 highlights the DC-link voltage response for both the proposed IHSF-LMS control scheme and the conventional LMS algorithm, with an acceptable range of 2% applied for DC-bus voltage settling. Analyzing the settling time and overall response in Figure 7, it becomes evident that the IHSF-LMS control scheme outperforms the conventional LMS in dynamic performance. The proposed design excels in key areas, including weight convergence, error minimization, reduced peak overshoot, faster rise time, improved settling time, and effective harmonic mitigation. The comparative results summarized in Table 2 further emphasize the superior performance of the IHSF-LMS controller over the conventional LMS, validating its effectiveness as a robust and efficient control strategy.

Table 2. A comparative study of the conventional algorithm with the proposed IHSF-LMS-based control scheme

Operations		LMS	IHSF-LMS
Type		Adaptive	Adaptive
Convergence		Slower	Faster than LMS
Complexity		Less	Less
Convergence of weight	Steady-state condition	Higher amplitude having sustained oscillations	Lower amplitude having sustained oscillations
	Unbalanced condition	Sustained oscillations	Faster convergent
THD analysis	Source voltage	25.53%	25.53%
	Load voltage	3.03%	1.61%
	Load current	2.05%	1.48%
Steady state error		More than IHSF-LMS	Significantly less than LMS
Max. overshoot (%Mp)		4.45%	2.92%
Rise time (tr s)		0.084 s	0.082 s
Settling time (t_s s)		0.135 s	0.118 s

A novel adaptive control scheme for dynamic voltage restorer (Tummala Kranti Kiran)
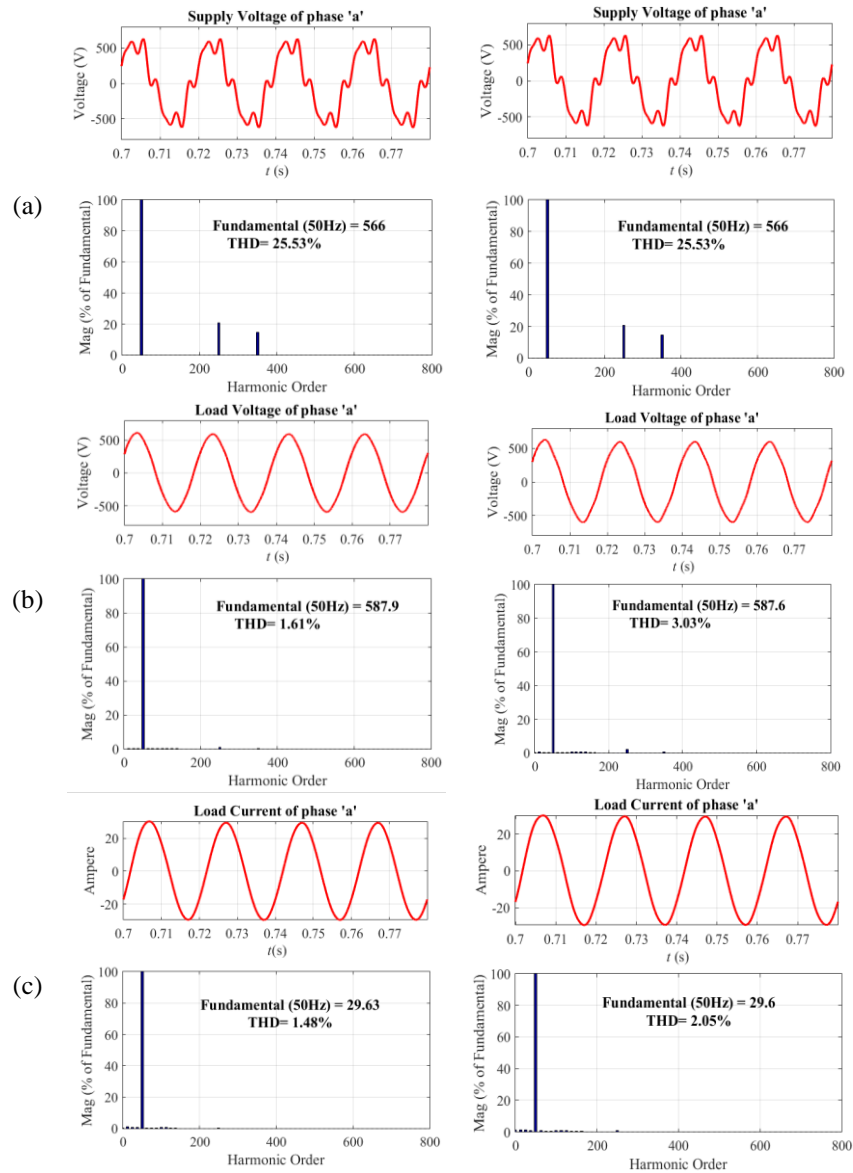
(a)

(b)

(c)

Figure 5. Harmonic analysis for (a) source voltage, (b) load voltage, and (c) load current,
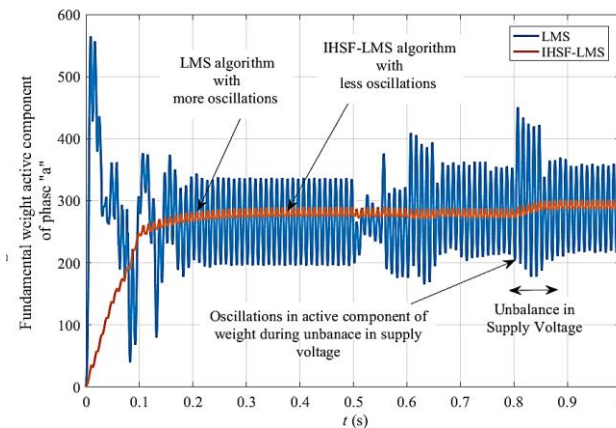with proposed IHSF-LMS and conventional LMS control scheme

Figure 6. Comparison between LMS and IHSF-LMS control scheme based on the fundamental active
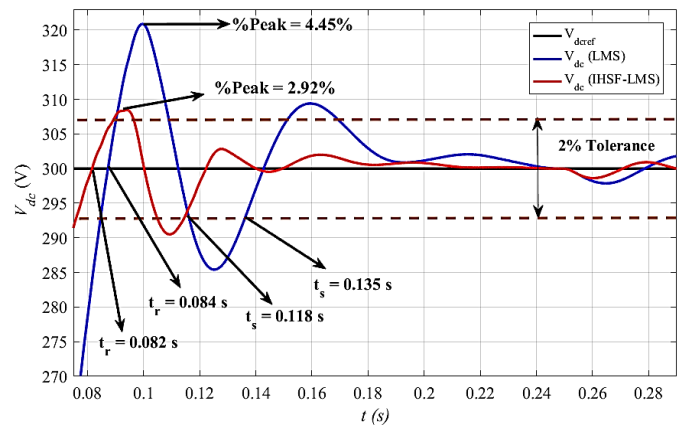component of phase 'a'

Figure 7. Response of DVR DC-link voltage with tuned PI controller gains:
(a) IHSF-LMS and (b) conventional LMS

6.   CONCLUSION

A 3P3W VSC-based DVR, integrated with the IHSF-LMS control scheme, underwent a comprehensive evaluation to assess its performance across diverse voltage conditions, including sag, swell, unbalance, and distortion in the supply voltage. The IHSF-LMS framework showcased superior adaptability, effectively tracking supply voltage variations while maintaining an optimal balance between convergence speed and misalignment. The results demonstrate a remarkable improvement in DVR functionality, delivering rapid convergence, enhanced robustness, and reliable compensation capabilities. Compared to the conventional LMS algorithm, the proposed IHSF-LMS control strategy achieved notable advantages, including reduced peak overshoot, quicker settling time, and shorter rise time. Notably, the load voltage's THD consistently adhered to IEEE-519-2014 standards, underscoring the algorithm's efficiency in harmonic suppression. This control scheme excelled in both dynamic and steady-state scenarios, reinforcing its reliability and robustness. System validation through MATLAB/Simulink further confirmed the significant enhancements in the DVR's overall performance, solidifying the IHSF-LMS control algorithm as a superior solution for power quality improvement. Parameters: system parameters for simulation: grid voltage with voltage anomalies- 3 phase, 415 V, 50 Hz; Load of 10 kVA with 0.82 p.f. (Lagg.); rating of injection-transformer = 11 kVA, 200/200 V; DC-link voltage (V_{dc}) = 300 V; DC bus capacitor (C_{dc}) = 3300 µF; Interfacing inductor (L_i) = 3 mH; passive ripple filter: $R_r = 6$ Ω and $C_r = 10$ µF; switching frequency of VSC: (f_s) = 10 kHz., adaptation constant $\gamma = 0.1$.

AUTHOR CONTRIBUTIONS STATEMENT

This journal uses the Contributor Roles Taxonomy (CRediT) to recognize individual author contributions, reduce authorship disputes, and facilitate collaboration.

Name of Author	C	M	So	Va	Fo	I	R	D	O	E	Vi	Su	P	Fu
Tummala Kranti Kiran	✓	✓	✓	✓	✓	✓		✓	✓	✓			✓	
Balakrishnan Rajagopal		✓				✓		✓	✓	✓	✓	✓		
Yerramilli Butchi Raju	✓		✓	✓		✓			✓		✓			✓

C : **C**onceptualization		I : **I**nvestigation		Vi : **Vi**sualization		
M : **M**ethodology		R : **R**esources		Su : **Su**pervision		
So : **So**ftware		D : **D**ata Curation		P : **P**roject administration		
Va : **Va**lidation		O : Writing - **O**riginal Draft		Fu : **Fu**nding acquisition		
Fo : **Fo**rmal analysis		E : Writing - Review & **E**diting				

CONFLICT OF INTEREST STATEMENT
Authors state no conflict of interest.

DATA AVAILABILITY
Data availability is not applicable to this paper as no new data were created or analyzed in this study.

REFERENCES

[1]   B. Singh, A. Chandra, and K. Al-Haddad, *Power Quality Problems and Mitigation Techniques*, vol. 9781118922. 2015. doi: 10.1002/9781118922064.

[2]   M. H. J. Bollen, "What is power quality?," *Electric Power Systems Research*, vol. 66, no. 1, pp. 5–14, 2003, doi: 10.1016/S0378-7796(03)00067-1.

[3]   A. Javadi, A. Hamadi, L. Woodward, and K. Al-Haddad, "Experimental Investigation on a Hybrid Series Active Power Compensator to Improve Power Quality of Typical Households," *IEEE Transactions on Industrial Electronics*, pp. 1–1, 2016, doi: 10.1109/TIE.2016.2546848.

[4]   A. Domijan, A. Montenegro, A. Keri, and K. Mattern, "Custom Power Devices: An Interaction Study," *IEEE Transactions on Power Systems*, vol. 20, no. 2, pp. 1111–1118, May 2005, doi: 10.1109/TPWRS.2005.846101.

[5]   S. Das, A. K. Pradhan, A. Kedia, S. Dalai, B. Chatterjee, and S. Chakravorti, "Diagnosis of Power Quality Events Based on Detrended Fluctuation Analysis," *IEEE Transactions on Industrial Electronics*, vol. 65, no. 9, pp. 7322–7331, Sep. 2018, doi: 10.1109/TIE.2018.2795559.

[6]   D. Rajasekara, S. Sekhar Das, and P. Vignesh, "Mitigation of Voltage Sags and Voltage Swells by Dynamic Voltage Restorer," in *International Conference on Advances in Recent Technologies in Communication and Computing*, 2011, vol. 5, no. 3, pp. 36–40. doi: 10.3923/ijepe.2011.139.143.

[7]   Changjiang Zhan *et al.*, "Dynamic voltage restorer based on voltage-space-vector PWM control," *IEEE Transactions on Industry Applications*, vol. 37, no. 6, pp. 1855–1863, 2001, doi: 10.1109/28.968201.

[8]   Changjiang Zhan, C. Fitzer, V. K. Ramachandaramurthy, A. Arulampalam, M. Barnes, and N. Jenkins, "Software phase-locked loop applied to dynamic voltage restorer (DVR)," in *2001 IEEE Power Engineering Society Winter Meeting. Conference Proceedings (Cat. No.01CH37194)*, vol. 3, pp. 1033–1038. doi: 10.1109/PESW.2001.917210.

[9]   K. Chandrasekaran and V. K. Ramachandaramurthy, "An improved Dynamic Voltage Restorer for power quality improvement," *International Journal of Electrical Power and Energy Systems*, vol. 82, pp. 354–362, 2016, doi: 10.1016/j.ijepes.2016.02.036.

[10]   P. Kanjiya, B. Singh, A. Chandra, and Kamal-Al-Haddad, "'SRF theory revisited' to control self-supported dynamic voltage restorer (DVR) for unbalanced and nonlinear loads," in *2011 IEEE Industry Applications Society Annual Meeting*, Oct. 2011, pp. 1–8. doi: 10.1109/IAS.2011.6074356.

[11]   P. Shukla and B. Singh, "Synchronization of Solar PV System to Grid with Enhanced Power Quality," in *2021 4th Biennial International Conference on Nascent Technologies in Engineering (ICNTE)*, Jan. 2021, pp. 1–6. doi: 10.1109/ICNTE51185.2021.9487702.

[12]   V. Deshpande Chinmay and V. Deshpande Chaitanya, "Optimum design of dynamic voltage restorer for voltage sag mitigation in distribution network," *International Journal of Power Electronics and Drive Systems*, vol. 10, no. 3, pp. 1364–1372, 2019, doi: 10.11591/ijpeds.v10.i3.pp1364-1372.

[13]   K. R. Patil and H. H. Patel, "Modified dual second-order generalised integrator FLL for synchronization of a distributed generator to a weak grid," in *2016 IEEE 16th International Conference on Environment and Electrical Engineering (EEEIC)*, Jun. 2016, pp. 1–5. doi: 10.1109/EEEIC.2016.7555824.

[14]   B. Singh, P. Jayaprakash, and D. P. Kothari, "Adaline-based control of capacitor supported DVR for distribution System," *Journal of Power Electronics*, vol. 9, no. 3, pp. 386–395, 2009.

[15]   H. M. M. Alhaj, N. M. Nor, V. S. Asirvadam, and M. F. Abdullah, "Power system harmonics estimation using LMS, LMF and LMS/LMF," in *2014 5th International Conference on Intelligent and Advanced Systems (ICIAS)*, Jun. 2014, pp. 1–5. doi: 10.1109/ICIAS.2014.6869521.

[16]   M. Srinivas, I. Hussain, and B. Singh, "Combined LMS–LMF-Based Control Algorithm of DSTATCOM for Power Quality Enhancement in Distribution System," *IEEE Transactions on Industrial Electronics*, vol. 63, no. 7, pp. 4160–4168, Jul. 2016, doi: 10.1109/TIE.2016.2532278.

[17]   J. R. S. Martins, D. A. Fernandes, F. F. Costa, M. B. R. Corrêa, A. J. Sguarezi Filho, and E. R. C. da Silva, "Optimized voltage injection techniques for protection of sensitive loads," *International Journal of Electrical Power and Energy Systems*, vol. 116, 2020, doi: 10.1016/j.ijepes.2019.105569.

[18]   C. V. Deshpande, R. Chilipi, and S. R. Arya, "Frequency Adaptive Enhanced Reduced-Order Generalized Integrator Control for Operation of DVR," in *2023 IEEE International Conference on Energy Technologies for Future Grids (ETFG)*, Dec. 2023, pp. 1–6. doi: 10.1109/ETFG55873.2023.10408206.

[19]   A. Khalifi, Q. Mayyala, N. Iqbal, A. Zerguine, and K. Abed-Meraim, "Adaptive algorithm based on a new hyperbolic sine cost function," in *2017 51st Asilomar Conference on Signals, Systems, and Computers*, Oct. 2017, pp. 812–815. doi: 10.1109/ACSSC.2017.8335459.

[20]   L. Lu, L. Chen, Z. Zheng, Y. Yu, and X. Yang, "Behavior of the LMS algorithm with hyperbolic secant cost," *Journal of the Franklin Institute*, vol. 357, no. 3, pp. 1943–1960, Feb. 2020, doi: 10.1016/j.jfranklin.2019.12.040.

[21]   J. Zeng, Y. Lin, and L. Shi, "A Normalized Least Mean Square Algorithm Based on the Arctangent Cost Function Robust Against Impulsive Interference," *Circuits, Systems, and Signal Processing*, vol. 35, no. 8, pp. 3040–3047, Aug. 2016, doi: 10.1007/s00034-015-0175-5.

[22]   C. Deshpande, R. Chilipi, and S. R. Arya, "A multi-convex composition of adaptive LMS filter-based control for dynamic voltage restorer with SSO-optimized PI gains," *Electrical Engineering*, Feb. 2024, doi: 10.1007/s00202-023-02119-4.

[23]   C. V. Deshpande, R. Chilipi, and S. R. Arya, "Modified fractional least mean square-based control scheme for dynamic voltage restorer to improve power quality," *Electrical Engineering*, vol. 106, no. 4, pp. 5069–5087, Aug. 2024, doi: 10.1007/s00202-024-02270-6.

[24] V. Deshpande Chinmay, V. Deshpande Chaitanya, and A. Deokar Sanjay, "Performance evaluation of dynamic voltage restorer based on transformer-based Z source inverter," *International Journal of Power Electronics and Drive Systems*, vol. 8, no. 3, pp. 1101–1108, 2017, doi: 10.11591/ijpeds.v8i3.pp1101-1108.
[25] S. Guan, Q. Cheng, Y. Zhao, and B. Biswal, "Robust adaptive filtering algorithms based on (inverse)hyperbolic sine function," *PLoS ONE*, vol. 16, no. 10 October, 2021, doi: 10.1371/journal.pone.0258155.

BIOGRAPHIES OF AUTHORS

Tummala Kranti Kiran is an Assistant Professor in the Department of Electrical Engineering at Sir C. R. Reddy College of Engineering, Eluru, Andhra Pradesh, India. He received his B.Tech. and M.Tech. degrees in Electrical Engineering in 2003 and 2006 respectively. He has been working as an assistant professor since 2007. He is, at present, the external research scholar of Annamalai University, Annamalainagar, Tamil Nadu, India. His research interests include power systems, power electronics, motor drives, and renewable energy. He can be contacted at email: krantikiran.tummala@gmail.com.

Balakrishnan Rajagopal is an Associate Professor in the Department of Electrical Engineering at Annamalai University, Annamalainagar, Tamil Nadu, India. He received his B.E. M.E., and Ph.D. Degrees in Electrical Engineering. He has been working as an associate professor since 2001. He published 10 papers in International Journals. His research interests include electrical machines, power electronics, IoT-based systems, renewable energy, high voltage engineering, and power systems. He can be contacted at email: ba_raj7278@rediffmail.com.

Yerramilli Butchi Raju is a Professor in the Department of Electrical Engineering at Sir C. R. Reddy College of Engineering, Eluru, Andhra Pradesh, India. He received his B.Tech, M.Tech., and Ph.D. degrees in Electrical Engineering in 1999, 2004 and 2012 respectively. He has been working as a professor since 2016. He published 15 papers in International Journals. His research interests include power system dynamics, power electronics, IoT-based systems, and renewable energy. He can be contacted at email: butchiraju.y@gmail.com.